

## Shock waves in rapid flows of dense granular materials: Theoretical predictions and experimental results

Shiva P. Pudasaini and Christian Kröner\*

*Department of Geodynamics and Geophysics, Steinmann Institut, University of Bonn, Nussallee 8, D-53115, Bonn, Germany*  
(Received 21 April 2008; revised manuscript received 22 July 2008; published 24 October 2008)

Strong shocks in rapid dense granular flows are studied theoretically and analyzed in detail to compare with benchmark experimental data. The experimental data includes particle image velocimetry measurements of dry granular flow following its continuous release from a silo. The rapidly moving material down the chute impinges on an obstruction wall erected perpendicular at the end of a long and steep channel. Impact leads to a sudden change in the flow regime from a fast moving supercritical thin layer to a stagnant thick heap with variable thickness. This flow configuration is particularly interesting because it is analogous to some hydraulic and aerodynamic situations. We present results about the depth and the velocity evolution and their comparisons with theoretical predictions associated with frictional granular flow equations incorporating anisotropic pressure conditions. These flow equations are integrated by implementing high-resolution nonoscillatory central differencing total variation diminishing schemes. The dynamical and geometrical effects of the flow will be discussed in detail. These include geometry evolution and depositions at supercritical and subcritical flows, the impact velocity, shock speed, its position and evolution, choice of numerical limiters, and the influence of friction angles on the dynamics and depositions. An excellent agreement between theoretical predictions and experimental observations will be demonstrated. These results can be applied to estimate impact pressures exerted by avalanches on defense structures or infrastructure along the channel and in the run-out zones, and to study the complex flow dynamics around the obstacles and in depositions when the mass comes suddenly to a standstill. Importantly, these results can form a basis for calibration of numerical simulations when strong shocks occur in granular flows.

DOI: [10.1103/PhysRevE.78.041308](https://doi.org/10.1103/PhysRevE.78.041308)

PACS number(s): 45.70.Ht, 47.57.Gc, 45.70.Mg

### I. INTRODUCTION

The flow of a granular avalanche is characterized by three different regimes: (i) the starting zone where rupture and fragmentation of the solid material occurs, (ii) the avalanching zone where the granular material reaches fast supercritical speed, and (iii) the run-out zone where the moving mass is decelerated and comes to a rather sudden standstill. In this paper, we are concerned with experimental and theoretical results on the run-out zone. Observations, both in the laboratory and nature, show that the rapid flow regime is characterized by fairly uniform velocity profiles with depth and dominant sliding at the base, while in the deposition regime and, in particular, in the transition region from the rapid flow into the deposition zone shocklike structures form, and an overall depth flow changes into a surface boundary layer flow, which, further downstream, quickly slows down and eventually settles. A first step towards modeling such complicated three-dimensional flows is to reduce it to two dimensions by studying the chute flow variant first and to obtain detailed experimental information on velocities and build up of deposition geometries. Moreover, computations performed with avalanche equations in rapid granular flows have shown that difficulties arise when such flows encounter obstructions or generate shocks [1–5]. Particularly notorious are configurations in which rapidly moving material impinges a wall. Therefore, we consider channel experiments by Pudasaini *et al.* [1] and simulate the flow by theoretical predictions.

The most important physical quantities in avalanche dynamics are the velocity distribution, evolution of the geometry, and the deposition profile [6–13]. From a structural engineering and planning point of view one must properly predict the flow field and estimate impact pressures on civil structures that may be hit by an avalanche in order to adequately design buildings, roadways, and rail transportation in mountainous regions. Equally important is to know the depth and velocity evolution of flowing granular materials through various channels in process engineering scenarios [14]. We consider the frictional granular flow theory [15–17]. These model equations, which describe the distribution of the avalanche thickness and the velocity, are a set of hyperbolic partial differential equations, and are numerically solved by implementing the high-resolution nonoscillatory central (NOC) differencing scheme with total variation diminishing (TVD) limiters [2,18,19]. However, the frictional avalanche theory and TVD schemes have not yet been implemented to study the generation and propagation mechanisms of strong shocks in rapid dense granular flows analogous to those of hydraulics, aerodynamics or gas dynamics, and comparison with the benchmark experimental data generated by using high-resolution particle image velocimetry (PIV) measurement system [1]. If there is good agreement between theory and experimental measurement of the height profile through the channel and in the deposit, then one can easily infer reliability and efficiency of the theory for practical use to predict the depth profile, velocity distribution, impact pressure, strain rate, and other relevant quantities as the avalanche slides down the channel.

Alternative constitutive equations have also been successfully applied for granular flows [20–26]. However, these au-

---

\*kroener@geo.uni-bonn.de

thors mainly focus their attention on the hydrostatic pressure, rough and mild slopes close to or below the internal friction angle where the flow takes place on the self-substrate. These flows are close to jamming, intermittent, slow, uniform, and steady, and could thus adjust their velocities. In contrast, we are dealing with different flow conditions where the flow takes place on steep and relatively smooth slope thus inducing rapid motion. Furthermore, we do not need the explicit knowledge of the critical slope of the free surface in the dynamic simulation of rapid flows. This is automatically taken into account by the pressure gradient. One could modify the basal drag as in Secs. 6.1.3, 10.2.3, and 12.3-4 in [2]. But our simulation results as compared with the experimental data do not demand for such modification.

## II. MODEL EQUATIONS AND NUMERICAL INTEGRATION

We consider the simple one-dimensional frictional granular flow equations on slope [2,15–17],

$$\frac{\partial h}{\partial t} + \frac{\partial}{\partial x}(hu) = 0, \quad \frac{\partial}{\partial t}(hu) + \frac{\partial}{\partial x}\left(hu^2 + \frac{1}{2}\beta h^2\right) = sh, \quad (1)$$

where  $t, x, h, u$  are the time, the coordinate along the slope, flow depth, and velocity, respectively, and  $\beta = gK \cos \zeta$ . Similarly,  $sh$  is the net driving force, where  $\zeta$  is the slope angle,  $s = g \cos \zeta (\tan \zeta - \tan \delta)$  is the net driving acceleration,  $g$  is the gravity acceleration, and  $K = 2 \sec^2 \phi (1 \mp \sqrt{1 - \cos^2 \phi \sec^2 \delta}) - 1$  is the earth pressure coefficient, where  $\delta$  and  $\phi$  are the internal and bed friction angles, respectively. The term  $\partial(0.5\beta h^2)/\partial x$  represents the pressure gradient. The source term,  $s$ , is the interaction of the medium with the surrounding, namely the gravity and the basal friction, and it makes the system inhomogeneous. The model equations (1), which comprise a hyperbolic system, can be rewritten in conservative form as  $\partial \mathbf{w} / \partial t + \partial \mathbf{f}(\mathbf{w}) / \partial x = \mathbf{s}$ , where  $\mathbf{w} = (h, m)^T$  is the vector of conservative variables. The momentum flux  $\mathbf{f}$  and the source term  $\mathbf{s}$  are given by  $\mathbf{f} = (m, m^2/h + \beta h^2/2)^T$ ,  $\mathbf{s} = (0, sh)^T$ . Numerical schemes solving these equations must be able to grasp the dramatically changing flow behavior from the supercritical to the subcritical state. Shock formation is an essential mechanism in granular flows on an inclined surface encountering an obstacle when the velocity becomes subcritical from its supercritical state. It is therefore natural to employ conservative high-resolution numerical techniques that are able to resolve the steep gradients and moving fronts often observed in experiments and field events but not captured by traditional finite difference schemes. The TVD-NOC differencing scheme with the Minmod limiter demonstrates the best numerical performance for simulating avalanche dynamics [2,14,18,27–30]. Our experimental results, presented in Sec. V, are better reproduced by Minmod limiter.

## III. EXPERIMENTAL CONDITIONS

Experiments were performed in a 10-cm-wide chute inclined at  $\zeta = 50^\circ$ , Figs. 1 and 2. Sidewalls and basal surface consist of 10-mm-thick transparent Plexiglas. All three sur-

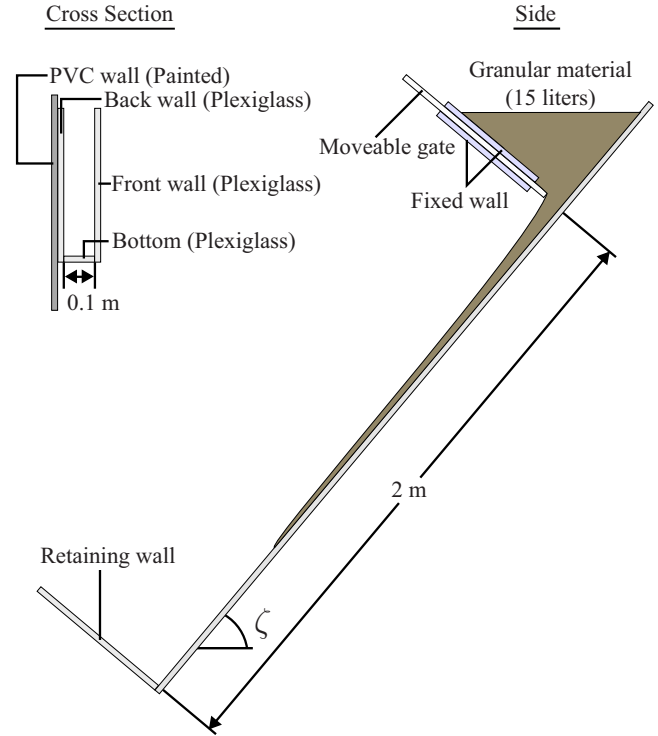


FIG. 1. (Color online) Side view and cross section of the chute with construction and dimensional details.

faces have friction angles with our materials of  $22^\circ (\pm 2^\circ)$  and lead to very limited boundary layer effects. The sidewise boundary layer thickness turned out to be very thin, and the corresponding friction was largely ineffective, i.e., motion was approximately plane (as viewed from the top). This is in agreement with the findings in [23–26] where it is shown that generally for  $\zeta > 30^\circ$  boundary layer effect with/without walls vanishes. Our PIV measurement shows almost no wall boundary effect for  $\zeta > 40^\circ$  and channel longer than 0.7 m [2]. At the top of the chute, a narrow rectangular silo with a plate gate is mounted perpendicular to the channel base. 15 l of quartz particles of about 4 mm mean diameter (mean of randomly chosen 50 particles) were used for our experiments.

After the release, the mass quickly acquires large velocities and forms a rather thin layer of rapidly moving material. The fast moving granular mass would, upon encountering the retaining wall erected perpendicular to the channel at 2 m distance downstream, form a stagnant deposit that accumulates mass close to the wall. As the flow of mass from the reservoir continues, a shocklike transition region moves backwards from the wall, gaining mass at supercritical speed from above. In the heap that is formed the velocities are by no means uniformly distributed with depth; they are rather largely restricted to the top surface boundary layer within and close to the granular jump transition region. More careful scrutiny reveals that at the heap surface avalanching flows rearrange the geometry to accommodate the slope close to the angle of repose, see Figs. 2 and 9. However, in this paper, we will not deal with the velocity shearing through depth. This will be the subject of a separate paper. Unless otherwise stated, the inlet height, velocity and inter-



FIG. 2. (Color online) Laboratory experiments of dry granular chute flows impinging an obstructing wall. Granular material is continuously released by opening the shutter of the silo (a). The material then moves rapidly down the chute and impinges on the obstructing wall forming shock (b). This leads to a sudden change in the flow regime from a fast moving supercritical thin layer to a stagnant thick heap with variable thickness and a surface dictated by the angle of repose typical for the material. Final deposition is shown in the (c).

nal and basal friction angle are  $h_s=6$  cm,  $u_s=0.37$  ms<sup>-1</sup>,  $\phi=33^\circ$ , and  $\delta=22^\circ$ , respectively. Also note that, the channel slope remains constant for each particular simulation or experiment but does not vary along the downhill as a function of the longitudinal coordinate  $x$ ; otherwise the channel slope would be called a variable one, i.e.,  $\zeta=\zeta(x)$ .

#### IV. STRONG SHOCK WAVES IN DENSE GRANULAR FLOWS

##### A. Numerical simulations of channel flows with various limiters

In this section, we will present several simulation results that will describe various scenarios of flows. Figure 3 represents a time series of granular flows just after the gate of the silo is opened until it comes to the final deposition. For ease,

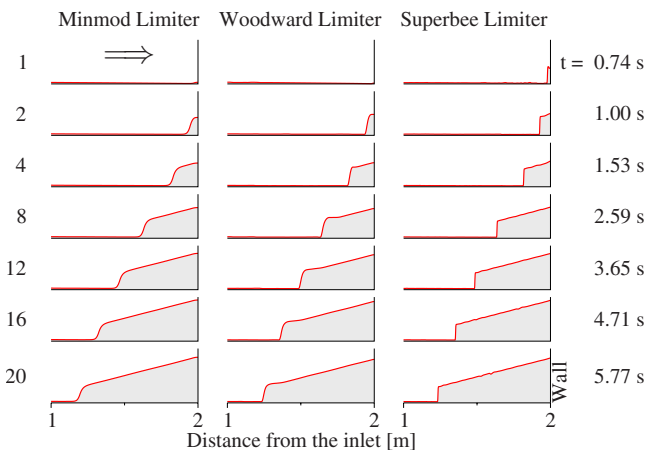


FIG. 3. (Color online) Numerical simulations of channel flows of granular materials impinging the front wall as indicated in the last panel of the right-hand column.  $\Rightarrow$  indicates the flow direction. Only the final 1 m length of the channel from the wall to the upstream direction is shown here. Panel numbers are indicated on the left-hand side and the corresponding times are indicated on the right-hand side. Simulations are performed with three different TVD limiters as indicated. Other physical parameters are  $\zeta=50^\circ$ ,  $h_s=6$  cm,  $u_s=0.37$  ms<sup>-1</sup>,  $\phi=33^\circ$ ,  $\delta=22^\circ$ .

unless otherwise stated, figures are plotted in the horizontal settings. Similarly, although in the experiments, the flow is from the top right-hand side to the bottom left-hand side, here in simulations the flows are from left to right. The mass is shown in gray and the free surface in red color. As soon as the moving front hits the wall a strong granular shock is immediately generated in panel 2 at time  $t=1.00$  s. The stagnant heap does not have constant depth, instead the depth is largest at the retaining wall and decreases as one moves towards the shock front. As the flow transits into the heap, the motion appears to be parallel to the S-shaped surface of the shock, strongly attenuated with depth and quickly coming to a standstill. The subsequent panels show how the rapidly moving material between the head gate and the growing deposited pile accumulates mass as long as the granular flux continues from above. In an analogy to aerodynamics or hydraulics, the transition region from the rapid, supercritical flow to the stagnant heap will be called a diffuse shock or a granular jump, “diffuse,” because of its considerable width (mainly for the left-hand column), comparable in size to the heap depth and much larger than a particle diameter.

We have simulated the flow with three different TVD limiters. From the theoretical point of view, the minmod limiter is the most diffusive, the superbee the most antidiffusive, and the woodward lies in between (see, Pudasaini and Hutter [2]). Since the flow of highly frictional granular material in very steep channels can generate strong shock fronts, while hitting the front wall, the validity of this argument can easily be checked with our simulation tests. The three columns in Fig. 3 display simulation result with the minmod, woodward, and superbee limiters, respectively. Comparing the three columns we observe that, in fact the above claim is true, which is a very important conclusion. With the superbee limiter, the shock front is almost perpendicular to the channel. With the woodward limiter, the front is slightly oblique with the normal of the channel base. Moreover, with the minmod limiter, all the shock fronts are a bit diffused from the beginning of its generation until the last panel. Note that, the minmod limiter is chosen in all simulations that follow in this paper.

##### B. Effect of the channel slope

We ran simulations for channel slope angles  $\zeta=15, 25, 30$ , and  $35^\circ$  see Fig. 4. For  $\zeta=15^\circ$ , after panel 8 ( $t=2.59$  s), the

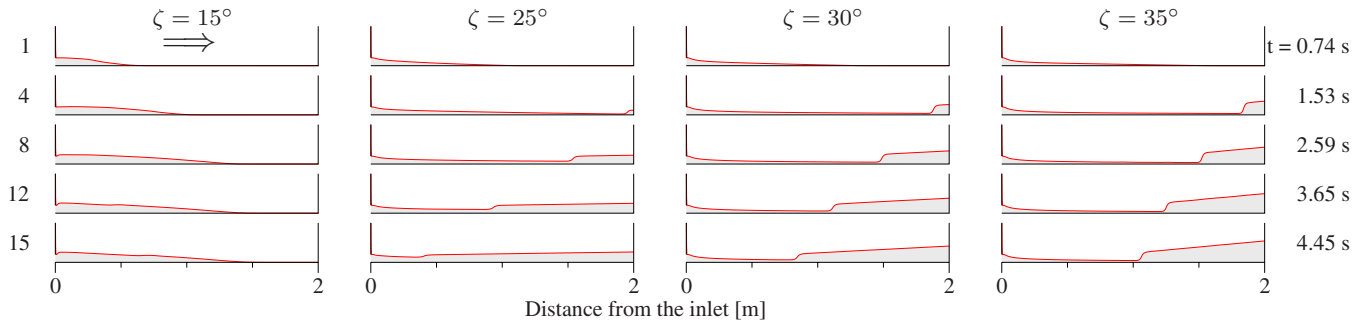


FIG. 4. (Color online) Effect of the channel slope on the dynamics of the shock front and the free-surface evolution of the depositions.  $\Rightarrow$  indicates the flow direction. Numbers on the left-hand side are the panel numbers in the simulation and those on the right-hand side show the corresponding times. Other physical parameters are  $h_s=6$  cm,  $u_s=0.37$  ms<sup>-1</sup>,  $\phi=33^\circ$ ,  $\delta=22^\circ$ .

flow front virtually does not move. The flow was mainly caused by the pressure of the mass in the silo, but also the gravity and the friction forces are active there. Moreover, after panel 4, there is a very small increase in the slope and the height of the free surface of the successive depositions due to the small and slow discharge of the granular mass from the silo gate. Since the slope of the channel is much lower than the angle of repose, the free surface of the deposit is close to the slope angle of the chute. Next, we consider  $\zeta = 25^\circ$ , therefore the slope angle is higher than the bed friction angle. Since  $\zeta > \delta$ ,  $s > 0$  the mass accelerates. For this, the front of the avalanche moves faster and hits the front wall at panel 4 ( $t=1.53$  s). Then a very small amplitude shock front is created which rapidly propagates upslope and finally diffuses, and the mass ceases to flow (after panel 15). Since the granular mass is frictional and the slope angle of the chute is still much below the material friction angle, the free surface of the deposited material is (almost) parallel to the channel bed.

For  $\zeta \geq 30^\circ$  the slope angle is either close to or higher than the material friction angle  $\phi$ . Pudasaini and Hutter [2] discuss with the help of PIV data that the flow may behave differently when the slope angle of the channel is below the internal friction angle than when it is above. To facilitate the analysis, we define the support, of the deposit, to be the area between the front wall and the shock front. The interesting result is that as  $\zeta$  increases, the granular mass moves with high momentum and kinetic energy so that the height of the deposit increases, and due to the mass balance requirements,

the support decreases, consequently the position of the shock front is farther away from the silo inlet at a given time. Also note that in these simulations, resolution of the shock front was possible due to the high-resolution shock capturing method. Another interesting point is that the thickness of the flowing mass depends strongly on the channel slope. For a given point in the channel, the flow depth (“granular graph”) increases as  $\zeta$  decreases. The same physical behavior is also observed in other simulations with  $h_s=4, 8, 10$  cm.

We have two important observations: (i) The lake-at-rest condition [31], which is satisfied for ideal fluids is not satisfied for frictional granular and geomaterials, because, in all depositions, the free surfaces are almost parallel to the bed which is inclined to the horizontal at  $15^\circ$  to  $50^\circ$ . (ii) The Coulomb friction balances the downslope component of gravity regardless of whether the material is in motion or not [32]. Therefore, the surplus  $s$  acts against the gradient of the free surface. In this situation, the flow could also be assumed to be in standstill. To analyze this, we set the net driving acceleration  $\mathbf{s}=\mathbf{0}$ . However, our simulation shows a considerable influence of the net driving force on the flow dynamics even in situations when  $\zeta < \delta$ , see Fig. 5. Consider the left-hand two columns, for  $\zeta=15^\circ$ . In fact, if we set  $s=0$ , then the dissipative friction force in excess to the gravity force ( $s < 0$ ) is neglected; the flow is nonaccelerating and the momentum transfer is only due to the free-surface (pressure) gradient  $\partial h / \partial x$ , and the frictional resistance is neglected. Therefore, the momentum transfer is unphysically large (Fig. 9 will support this claim, because our simulation with  $s \neq 0$

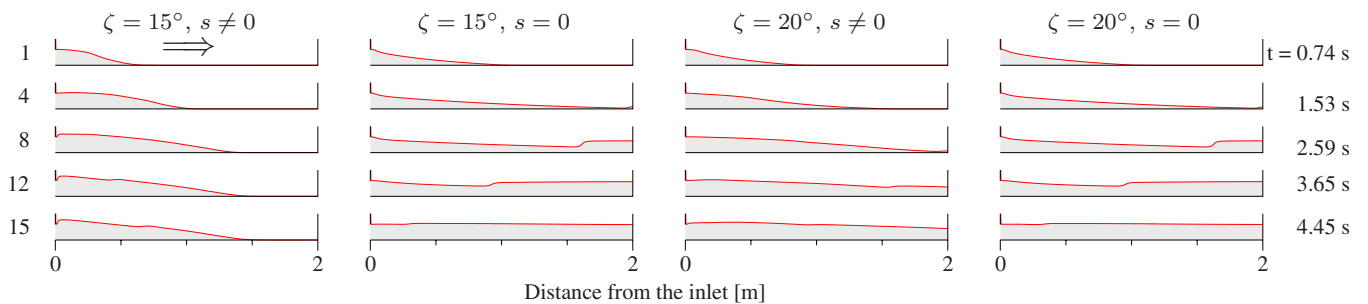


FIG. 5. (Color online) Effect of the net driving force on the dynamics of the shock front and the free-surface evolution of the depositions.  $\Rightarrow$  indicates the flow direction. Numbers on the left-hand side are the panel numbers in the simulation and those on the right-hand side show the corresponding times. The vertical axis is amplified by a factor of 2. Other physical parameters are  $h_s=6$  cm,  $u_s=0.37$  ms<sup>-1</sup>,  $\phi=33^\circ$ ,  $\delta=22^\circ$ .

fits very well with experiments) so that the flow already hits the front wall at panel 4 ( $t=1.53$  s); relatively strong shock is formed, which propagated upslope and finally the flow ceases at panel 15 ( $t=4.45$  s). However, with physically correct net driving acceleration,  $s \neq 0$ , there is an interplay between the deformation caused by the surface gradient, and the momentum transfer counteracted by the excess friction force due to  $s < 0$ . The flow ceases (almost) at panel 8 ( $t=2.59$  s) and never hits the front wall. Next, we consider the right-hand two columns of Fig. 5 with  $\zeta=20^\circ$ . For  $s=0$ , the momentum flux created by the surface gradient is not controlled by friction so that the flow already hits the wall at panel 4 ( $t=1.53$  s), a relatively strong shock is formed that propagates upslope and, finally, the flow ceases at panel 15 ( $t=4.45$  s) with free surface being parallel to the bed. However, with the physically correct force balance,  $s \neq 0$ , the flow hits the front wall only at panel 8 ( $t=2.59$  s), the shock is very weak, the free surface of the final deposition is not parallel to the bed. Therefore, the intensity of the shock depends on the amount of the momentum flux: The larger the momentum flux the higher the shock intensity.

### C. Role of the internal and bed friction angles

One of the material parameters, responsible for the fluidization of the granular material is the internal friction angle,  $\phi$ . The fluidization must be responsible for the shape and position of the deposited heaps. For these reasons, here we present simulations for  $\phi=30^\circ, 35^\circ, 40^\circ$ , and  $45^\circ$  in Fig. 6, left-hand column, which shows, as the internal friction angle  $\phi$  decreases, the fluidity increases. So, the heights of depositions increase but the supports decrease. The physical reason for this is simple: For smaller  $\phi$ , material is more fluidized, mass moves faster and can easily deform and ride on the surface of the already buried mass. But, once supercritically flowing mass rises up and rides on the stagnant heap through the shock, it must again slide down the surface of the stationary heap, to approach the angle of repose. This is the reason for larger heights at the retaining wall and smaller supports of the deposited materials for smaller values of  $\phi$ . As the internal friction increases, the granular fluidity decreases, flow is relatively slow, and material cannot so easily deform and ride to the free surface through the shock. Consequently, deposition heights are smaller and due to the mass balance requirements, the supports must be larger. Surprisingly, viewing from the inclined configuration, the free surfaces of depositions are higher for lower values of  $\phi$ . The angles of the free surfaces, in all cases, are close to their corresponding angles of repose, in conformity with the laboratory experiments [1]. In conclusion, the forms and positions of depositions are strongly influenced by the internal friction angle, a fact never explored and discussed in the literature. It is always argued that the dynamics and deposits of the granular flows are not sensitive to  $\phi$  [2]. That argument is perhaps true only for smooth changes of flow variables into depositions but when abrupt changes occur,  $\phi$  plays an important role in the dynamics and depositions of the granular mass. The reason here is the compaction of the already buried mass and the fluidity related to  $\phi$  that deter-

mines the slope of the deposition and thus its support. Note that, some authors even neglect the effect of  $\phi$  by setting  $K=1$ , and assume that the granular material behaves as an ideal fluid with friction only at the base. Our finding demonstrates a strong dependence of the dynamics and depositions of granular flows on the internal angle of friction.

It was demonstrated in [2], for relatively smooth flow configurations that, the run-out distance and the final depositions are sensitive to the bed friction angle but not to the internal friction angle. However, in our present simulation it is found that the dynamics and depositions are not influenced substantially by the bed friction angle, but on the contrary, by the internal friction angle. Figure 6, right-hand column, depicts plots for various bed friction angles,  $\delta=10, 15, 20$ , and  $25^\circ$ . For smaller values of  $\delta$ , due to the fact that less energy is dissipated in friction and that it is easier to lubricate, material slips easily along the bed. The material with small bed friction angle is deposited first followed by its larger values. However, the forms and positions of depositions are almost unchanged. Therefore, the important information here is that, for the present configuration, the dynamics is dominated by the internal friction angle, but not by the bed friction angle, in contrast to the previous conclusions [27,33].

The results of Fig. 6 are obvious to explain now that they are known. The sensitivity of the deposition to variations in  $\phi$  is likely due to the fact that the deposit region has no motion at the base but some motion in the interior. The contact pressure at the base is more or less constant in the deposit, but there is only motion within the diffusive regime. So, if one changes the value of  $\delta$ , almost nothing happens. However, downslope normal pressure  $\sigma_x$  is still effective and changes with  $\phi$  in the diffusive regime. The passive  $\sigma_x$  operates at the end of the diffusive shock regime. At the shock position or slightly before it,  $\sigma_x$  takes the active value. Therefore, this pressure difference generates the backward motion of the shock, and the difference grows with growing  $\phi$ .

### D. Inlet velocity and height

We used different inlet velocities from the silo gate. The corresponding results, plotted in Fig. 7, left-hand column,

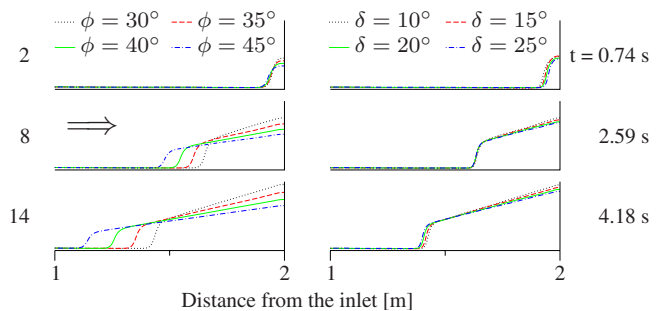


FIG. 6. (Color online) Influence of the internal (left-hand side, where  $\delta=22^\circ$  is fixed) and bed (right-hand side, where  $\phi=33^\circ$  is fixed) friction angle on the dynamics and depositions of granular flows in a steep rectangular channel impinging the frontal wall. Numbers on the left are the panel numbers in the simulation and those on the right-hand side show the corresponding times.  $\Rightarrow$  indicates the flow direction. Other physical parameters are  $\zeta=50^\circ$ ,  $h_s=6$  cm,  $u_s=0.37$  ms $^{-1}$ .

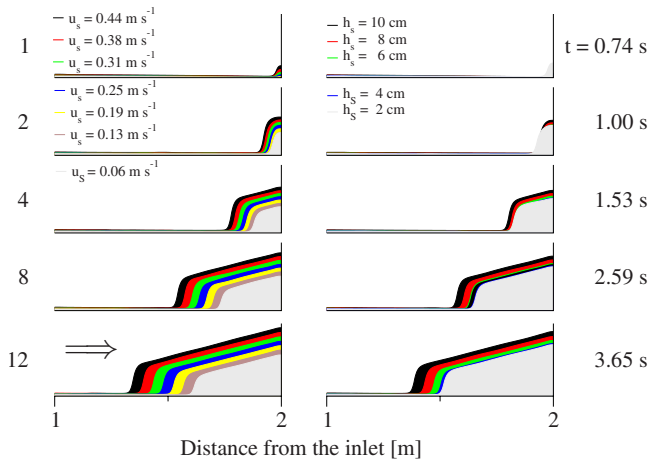


FIG. 7. (Color online) Influence of the inlet velocity (left-hand side) and the inlet height (right-hand side) on the dynamics and deposits of the granular flows in a steep rectangular channel impinging a front wall.  $\Rightarrow$  in the last panel of the left-hand column indicates the flow direction. Inlet velocities and inlet heights at the silo gate are indicated by  $u_s$  and  $h_s$ , respectively. For left-hand side,  $h_s=6$  cm, for right-hand side,  $u_s=0.37$   $\text{ms}^{-1}$ . The other parameters are  $\zeta=50^\circ$ ,  $\phi=33^\circ$ ,  $\delta=22^\circ$ .

show that the shapes of the depositions are exactly the same. The only changes are the times of depositions. In simulations with higher inlet velocity, because of the higher mass flux, the avalanche front hits the front wall earlier, thus forming the deposition earlier in time than the depositions associated with the smaller inlet velocities. Simulation results are presented in Fig. 7, right-hand column, for different inlet heights. Since the dynamics is described by the mass flux, the results are analogous to the left-hand column. The forms of the depositions are the same; higher inlet flow is deposited first followed (as measured by the deposited volume at the same time) by lower inlet height flows. However, ultimately, all the deposition graphs coincide. But, in contrast to the inlet velocity, the deposited mass does not vary linearly with inlet heights but seems to diverge.

### E. Stratification in granular deposition

Successive release of different granular materials from the silo form a stratified deposition. Deposited layers are such that, if the material of type 1 is released first followed by the material of type 2, then the material of type 1 is deposited first followed by material of type 2, and so on. This forms a strata from the basal surface to the top of the deposited body. Such phenomena can be observed in nature if one material is followed by another, due to successive avalanches or debris flows or if the eroded weak material of different type follows the main material body. So, such a study is important in geomorphology and landscape formation. For example, the deposit of a pyroclastic flow due to the volcanic eruption of Mt. St. Helens (1980) created such profile in which one complete flow unit was under and overlaid by other flow units, each corresponding to the passage of a pyroclastic flow [2]. Alternatively, in pharmaceutical or chemical industries, different granular and powder substances may have to be trans-

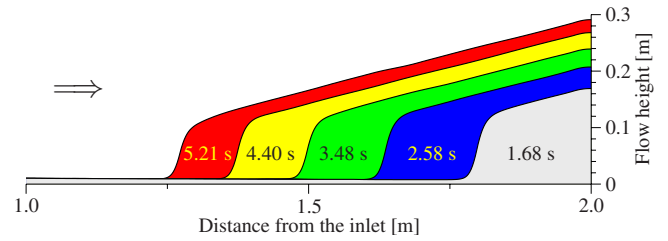


FIG. 8. (Color online) Stratified deposition generated by the flow of differently colored monodispersed granular material in a steep rectangular channel as the material impinges the frontal wall. Each material of 3 l (total 15 l) is released successively from the silo gate in sequence of gray, blue, green, yellow, and red and is deposited correspondingly. Other physical parameters are  $\zeta=50^\circ$ ,  $h_s=6$  cm,  $u_s=0.37$   $\text{ms}^{-1}$ ,  $\phi=33^\circ$ ,  $\delta=22^\circ$ .

ported successively and deposited accordingly. As discussed before, the form, slope, and location of deposition mainly depends on the internal friction angle of each material. Figure 8 shows the formation of strata of a differently colored monodispersed granular material released one after another according to their color and volume. This way, the stratified layers in the deposition can be constructed from our simulation.

### V. COMPARISON OF SIMULATIONS WITH RESULTS FROM PHYSICAL MODEL TESTS

In the present paper, we are mainly interested in understanding the transitional behavior of rapid granular flow from a supercritical to subcritical state on a steep slope. We wish to show how our model and numerical simulation technique can be used to study this strong transition, shock formation, and propagation in dry and cohesionless granular flows encountering obstacles and compare the results with laboratory experiments.

For this reason, we deal with and reproduce Experiment No. 3 of Pudasaini *et al.* [1]. The evolution of the pile buildup for the motion of quartz grains through the opening gate with the 6 cm gap is shown in Fig. 9. The following qualitative features are evident from the experiments: At the instant of first particle impingement on the retaining wall, there is violent bouncing that becomes lesser as the heap is formed. The stagnant heap in the experiments does not have constant depth; the depth is largest at the retaining wall and decreases approximately linearly as one moves towards the shock front. The shock is diffuse, i.e., the transition from the approaching supercritical flow with small height to the stagnant heap with large height is not abrupt but smooth with a characteristic S-shaped profile. In the supercritical regime above the stagnant heap, the velocity appears to be forward only, i.e., parallel to the basal surface, and there seems to be no variation of the speed with depth; plug flow seems to prevail. As the flow transits into the heap, the particle motion appears to be parallel to the S-shaped surface, strongly attenuated with depth and quickly coming to a standstill with increasing distance from the free surface into the heap. This boundary layer behavior is typical and influences the local shape of the heap surface. The second snapshot shows the

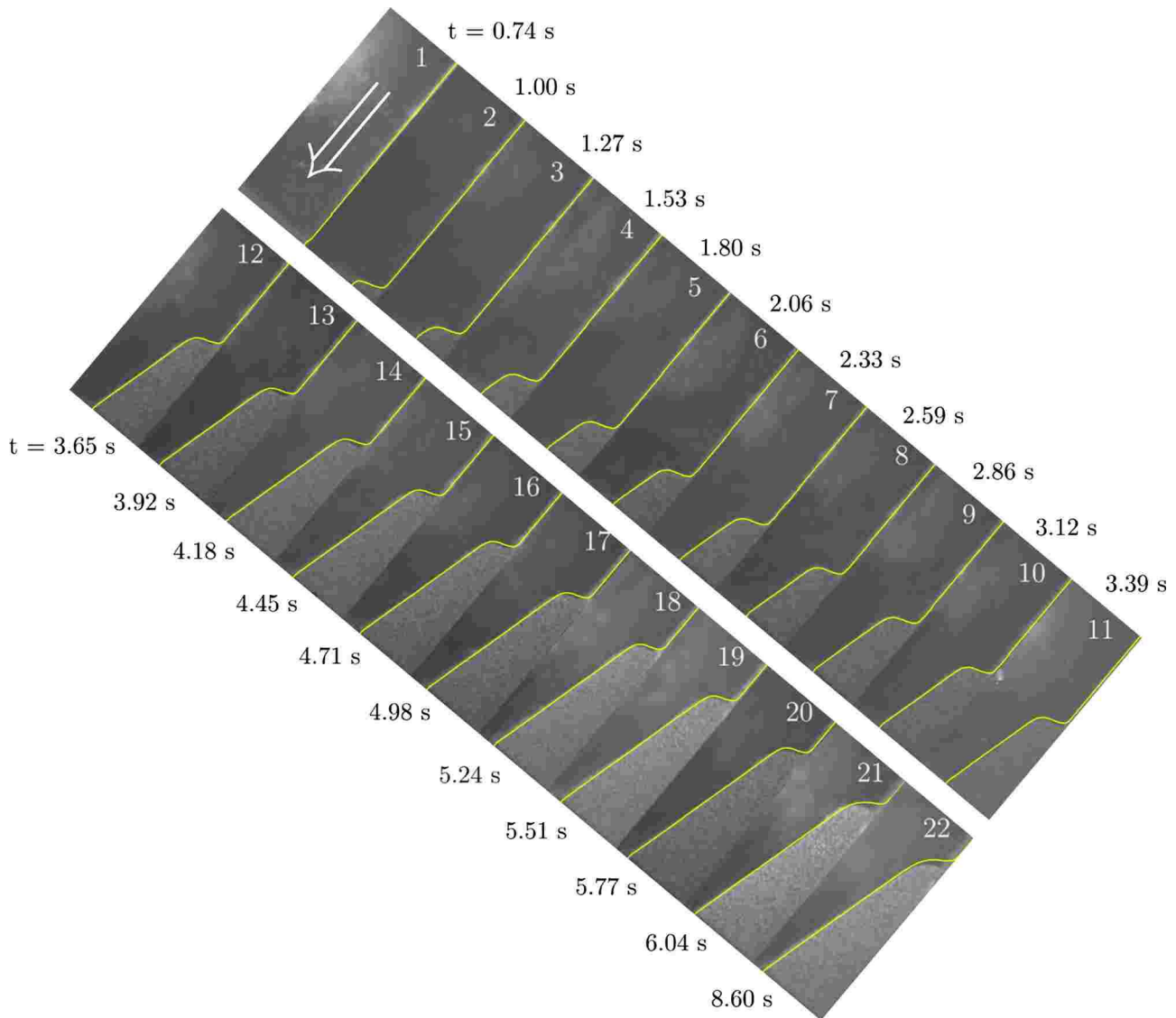


FIG. 9. (Color online) The solid dark gray filled graphs are the experimental snapshots of the rapidly flowing granular material (151 quartz sand) down the steep rectangular channel encountering the retaining wall erected 2 m below the opening gate of the silo. The 22 photographs are taken by the CCD camera of the PIV system. Only the lower 1 m of the channel adjacent to the front wall is shown here.  $\Rightarrow$  indicates the flow direction. The material has come to deposition in panel 20 and in the following two panels there is only free-surface migration and rearrangement of particles to maintain the angle of repose. The yellow lines are the evolution of theoretical predictions of the free surface and deposition. Other physical parameters are  $\zeta=50^\circ$ ,  $h_s=6$  cm,  $u_s=0.37$  ms $^{-1}$ ,  $\phi=33^\circ$ ,  $\delta=22^\circ$ .

flow in the configuration when the front of the granular material impinges on the retaining wall. The subsequent photographs show how the rapidly moving material between the head gate and the growing deposited pile accumulates mass as long as the granular flux continues from above. Visual inspection of the experiment shows that the rapid flowing material is climbing the deposition heap and quickly comes to rest as the top of the frontal zone is reached. In an analogy to aerodynamics or hydraulics, the transition region from the rapid, supercritical flow to the stagnant heap will be called a diffuse shock or a granular jump. In the last three panels 20–22 of Fig. 9, the flux is declined to zero and granular migration along the free-surface takes place; finally this surface is close to the angle of repose in panel 22, which in this case is equal to the internal angle of friction  $\phi=33^\circ$ .

#### A. Evolution of geometry and depositions

In rapid granular flows, it is very difficult to experimentally determine the actual flow depth in the inclined long channel because the flow is sheared immediately below the silo gate and is quickly thinning and accelerating. Since the opening of the head gate is only 6 cm and the travel distance is 2 m, the flow depth at the lower end of the channel will be only some particle diameters. However, accurate knowledge of the flow depth is very important. It is more meaningful and relatively easy to compare the buried mass and evolution of free surfaces of depositions between theory and experiments. Then, one can easily infer the dynamics of the flow through the entire channel length. Comparison of the evolution of the height fields between the simulation and the laboratory experiments are presented in Fig. 9. There is an excel-

lent agreement between the theoretical prediction and the measurement data. Although there is a perfect fit of the simulation result with the major part of the free-surface profile of the experimental measurement, little discrepancy is observed in the vicinity of the shock front in the last two panels. If we analyze the flow from the physical point of view, the buried mass behind the shock front is compacted due to the momentum transfer and the kinetic energy. Once it is compacted, due to the interlocking induced by the rough, angular, and irregular particle surfaces, the shape of the front stays more or less unchanged as a S form [1]. This form is preserved in all panels both for experiments and numerical simulations. Moreover, we could surprisingly simulate these results without entrainment mechanisms [34–36].

### B. Influence of the earth pressure coefficient

Here we analyze the effect of the earth pressure coefficient,  $K$  (see Sec. II), which quantitatively takes into account the two different modes of deformations; the extensional and contractional; on the dynamics and deposition of rapid granular flows [28]. Mechanically, the soil or sand is strong during compaction (passive mode) and weak during extension (active mode). The fact is that, the soil or sand can resist huge compressional stress but, on the contrary, these materials are very weak against extensional loads. This is the reason why the pressure coefficients are much higher than unity (the hydrostatic pressure), typically 5 times larger than the hydrostatic pressure, during compression, but much less than unity, typically 0.5 times smaller than the hydrostatic pressure, when the mass is extending [2]. Such amplification, or downplaying of the surface parallel normal pressures are included in the model equation (1) through the parameter  $\beta$  [17]. For ideal anisotropic fluids, which do not show normal stress effect,  $K=1$ .

Numerically, the earth pressure coefficient is the parameter which controls the flux. This is a fact which is not yet discussed in the literature of granular flow simulation. If the flux is not controlled physically correctly, numerical simulation results cannot be applied to real-world problems (like hazard mitigation and planning). To make things clear, we consider three different cases, see Fig. 10: (i) The frictional material with friction parameters and the earth pressure coefficient as considered in Sec. II. This corresponds to the (dotted) dark lines. As we have seen in Fig. 9, this accurately describes the flow dynamics and the depositions. (ii) Frictional material, but  $K=1$ , i.e., hydrostatic lateral pressure; (solid) green lines. In this case, the material flux is much higher than in reality. Therefore, due to unphysically induced higher momentum, the deposited mass is pushed too much to the wallside. This results in a dramatic increase in the pile depth and dramatic corresponding decrease of the support of deposited mass. (iii) Ideal fluid, no friction and  $K=1$ , (dashed) red lines. This is the worst case scenario. Here, not only the flux is highly amplified, but also the friction (e.g., basal friction) is neglected. This further amplifies the momentum and results in the highest depth profile and the shortest support in all time sequences. In this case, since the material is not frictional, the final deposition profile is almost

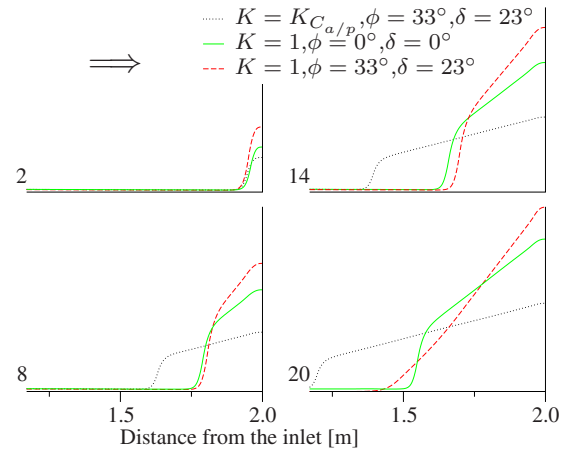


FIG. 10. (Color online) Influence of the earth pressure coefficient on the dynamics and depositions of the granular flows in a steep rectangular channel impinging the frontal wall. Numbers are the panel numbers in the simulation.  $\Rightarrow$  indicates the flow direction. Other physical parameters are  $\zeta=50^\circ$ ,  $h_s=6$  cm,  $u_s=0.37$  ms $^{-1}$ .

horizontal, thus satisfying the lake-at-rest criterion. This indicates the consistency of our model and the numerical simulation. Therefore, we conclude the following: In a rapid granular flow down a steep chute impinging on a rigid wall, the earth pressure coefficients are very important mechanisms to physically control the flux and accurately describe the dynamics and depositions.

### C. Shock position and maximum velocity

It is also important to know the shock position in time because this information is needed to determine the stagnation pressure. The shock position (indicated by a “ $\times$ ” in the inset of the corresponding figure) can be realized as the position of the maximum velocity as measured by the PIV system just in front of the transition. Figure 11 (top) depicts an excellent agreement between the measured shock position and its theoretical counterpart. This figure shows that the shock position propagates upslope (almost linearly) along the channel as a concave (upward) function of time.

In mountainous regions prone to avalanche or debris flows, civil engineers must know the impact pressures that can be induced by possible natural events. The wall of a house or any other infrastructure facing the slope of a mountain must be able to withstand the impact pressure associated with such natural events so as to reduce any casualties. The PIV measurement technique is useful to determine the velocity distribution, particularly the impact velocity in granular flows hitting an obstruction. The maximum velocity arises either at the instance when the flow hits the wall or in the subsequent images just in front of the shock. In Fig. 11 (bottom) the maximum velocity versus the distance from the inlet is plotted. The largest velocity, 4.1 ms $^{-1}$ , is seen at the instant when the flowing mass hits the front wall (panel 2, Fig. 9). The maximum velocity first decreases gently then more rapidly, and finally the decrease is less rapid again. It indicates development and disappearance of small surges in the granular flows in the narrow rectangular channel (see, [1]

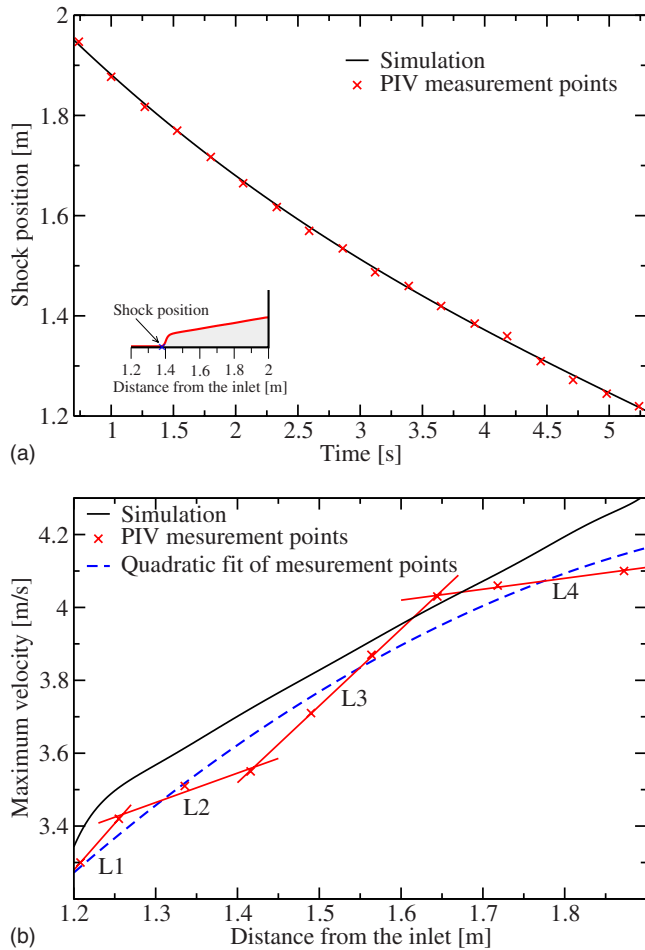


FIG. 11. (Color online) Top: Shock position; comparison between the laboratory and theoretical prediction of rapid granular flows down a steep rectangular channel impinging a frontal wall. The solid curve shows the numerical prediction and “x” denotes the PIV measurement points. The shock position is indicated in the inset. The vertical axis is the distance from the inlet and the wall is at 2 m. Bottom: Maximum velocity; comparison between the laboratory and theoretical prediction of rapid granular flows down a steep rectangular channel impinging the frontal wall. The line represents the maximum velocity obtained from the simulation, “x” denotes the PIV measurement points and the dashed line is its quadratic fit. Other physical parameters are  $\zeta=50^\circ$ ,  $h_s=6$  cm,  $u_s=0.37$  ms $^{-1}$ ,  $\phi=33^\circ$ ,  $\delta=22^\circ$ .

for likely causes of surges). Finally, the maximum velocity drops to 3.28 ms $^{-1}$ ; compare with the 20th frame in Fig. 9. So, the maximum velocity decreases almost linearly, but with some disturbances, as the shock front travels upslope. We define the impact velocity to be the velocity immediately before the hydraulic jump where the flow height is minimal. The maximum velocity occurs only some millimeter distance upstream of the channel from the shock front. As seen in Fig. 11 (bottom), there is good agreement between the theoretical prediction and the PIV measurements of the maximum velocity along the channel length.

Careful investigation indicates that there are four different flow behaviors in the downstream as denoted by four lines, L1, L2, L3, and L4 connecting the neighboring experimental

points with similar linear behaviors. The line L1 represents the flow relatively close to the silo inlet so that there is still a considerable flow depth and the pressure generated by the material load plays a significant role to increase the maximum velocity, although linearly. Shortly after that the flowing layer becomes thinner, the basal friction plays a dominant role so that the speed of the avalanche front cannot increase as before and it decelerates a bit, line L2. However, as soon as the front passes the distance of about 1.45 m, due to the very steep slope of the channel, the flow again gets momentum, line L3. The front accelerates rapidly again with a constant acceleration. Finally, as the flow front reaches the downslope distance of about 1.65 m, the front decelerates. The line L4 could be the indication of the steady-state flow situation as anticipated and discussed by many people [2,37]. Yet, we should also mention that, the sudden drop of the maximum velocity can also be attributed to the abrupt deposition of the mass that is very close to the position of the maximum velocity, through the shock. However, the global tendency of the experimental data as represented by the dashed line of quadratic fit agrees very well with our simulation, the solid line.

## VI. DISCUSSIONS AND SUMMARY

In this paper, we considered laboratory experiments of dry granular chute flows down steep slopes impinging an obstructing wall as a benchmark problem. We have implemented the frictional avalanche theory and conservative high-resolution TVD-NOC numerical schemes to study the generation and propagation mechanisms of strong shocks in rapid dense granular flows analogous to those of hydraulics, aerodynamics or gas dynamics, and comparison with experimental data generated by using PIV measurement system. To our knowledge, such results have not been presented before by making direct comparisons with the theoretical predictions.

We have simulated the flow with three different TVD limiters. “From the theoretical point of view, the minmod limiter is the most diffusive, the superbee the most antidiffusive, and the woodward lies in between.” Since the flows of highly frictional granular material in very steep channels can generate strong shock fronts, while hitting the front wall, the validity of this argument could be checked by our simulations. We observed that, in fact this claim is true. Since the flow behaves differently when the slope angle of the channel is below the friction angle than when it is above, we ran simulations for different channel slopes. The interesting result is that as the channel slope increases, the height of the deposit increases and the support of the deposit decreases, consequently the position of the shock front is farther away from the silo outlet. Similarly, the thickness of the flowing mass depends strongly on the channel slope. For a given point in the channel, the flow depth or the “granular graph” increases as the slope angle decreases. We have drawn two important observations: First, the lake-at-rest condition is not satisfied for frictional granular materials, because the free surfaces of depositions are not horizontal. Second, there is a considerable influence of the net driving force on the flow

dynamics even in situations when the slope angle is below the basal friction angle. Therefore, there is an interplay between the deformation caused by the surface gradient and the momentum transfer counteracted by the excess friction force due to nonvanishing net driving acceleration: The larger the momentum flux the higher the shock intensity.

Our simulations with different internal friction angles show that they are responsible for the fluidization of the granular material, which in turn determines the shape and position of the deposited heaps. For smaller internal friction angle, material is more fluidized, mass moves faster, it can easily deform and ride on the surface of previously buried mass, and heights of depositions increase while the supports decrease. Therefore, the forms and positions of depositions are strongly influenced by the internal friction angle, a fact never explored in the literature. For relatively smooth topographies the run-out distance and the final depositions are sensitive to the bed friction angle but not to the internal friction angle. However, our present study reveals that the dynamics and depositions are not influenced substantially by the bed friction angle, but by the internal friction angle. Since the dynamics are described by the mass flux, the change in inlet velocity and height produce similar results in which the shapes of depositions are exactly the same. The structure of the shock front and the deposition geometry as a whole depend on the choice of the TVD limiter as well as the physical parameters, the internal friction angle and the (anisotropic) longitudinal earth pressure coefficient, which, in fact, depends on the two material parameters, the internal and the bed friction angles, respectively. Moreover, our configuration is suitable to study stratification in granular deposition. Successive release of different granular materials from the silo results in a stratified deposition. Such phenomena can be observed in nature (geomorphology and landscape formation) if one material is followed by another.

Next, we consider comparison of simulations with results from physical model tests. In rapid granular flows, it is very difficult to experimentally determine the actual flow depth in the inclined long channel because the flow is sheared immediately below the silo gate. Accurate knowledge of the flow depth is very important for the study of the dynamic behavior of the flow. We have demonstrated that there is an excellent agreement between the theoretical prediction and the measurement data on the evolution of geometry and deposition. Although the use of the earth pressure coefficient is quite common in soil mechanics and geotechnics to quantitatively account for different modes of deformation, it is also argued that the granular pressure can be assumed hydrostatic. The present study reveals that, the earth pressure coefficients are very important mechanisms to physically and numerically control the flux and accurately describe the flow dynamics and depositions of granular masses. Our simulation shows an excellent agreement between the measured shock position and its theoretical counterpart. The shock position propagates upslope along the channel as a concave function of time. Finally, there is good agreement between the theoretical prediction and the PIV measurements of the maximum velocity along the channel length. This proves the applicability of the theory and efficiency of the employed numerical method and establishes a nice and strong correlation among theory, numerics, and experiments.

#### ACKNOWLEDGMENTS

We thank the German Research Foundation (DFG) for the financial support through Contract No. PU 386: Transition of a granular flow into the deposit. We are grateful to K. Hutter for fruitful discussions.

- 
- [1] S. P. Pudasaini, K. Hutter, S.-S. Hsiau, S.-C. Tai, Y. Wang, and R. Katzenbach, *Phys. Fluids* **19**, 053302 (2007).
  - [2] S. P. Pudasaini and K. Hutter, *Avalanche Dynamics: Dynamics of Rapid Flows of Dense Granular Avalanches* (Springer-Verlag, Berlin, 2007).
  - [3] J. M. N. T. Gray and X. Cui, *J. Fluid Mech.* **579**, 113 (2007).
  - [4] J. M. N. T. Gray, Y.-C. Tai, and S. Noelle, *J. Fluid Mech.* **491**, 161 (2003).
  - [5] K. M. Hákonardóttir, A. J. Hogg, T. Jóhannesson, and G. G. Tómasson, *J. Glaciol.* **49**, 191 (2003).
  - [6] A. Mangeney, F. Bouchut, N. Thomas, J. P. Vilotte, and M. O. Bristeau, *J. Geophys. Res.* **112**, F02017 (2007).
  - [7] A. Mangeney-Castelnaud, F. Bouchut, J. P. Vilotte, E. Lajeunesse, A. Aubertin, and M. Pirulli, *J. Geophys. Res.* **110**, B09103 (2005).
  - [8] A. K. Patra *et al.*, *J. Volcanol. Geotherm. Res.* **139**, 1 (2005).
  - [9] E. B. Pitman and L. Le, *Philos. Trans. R. Soc. London, Ser. A* **363**, 1573 (2005).
  - [10] E. B. Pitman, C. C. Nichita, A. Patra, A. Bauer, M. Bursik, and A. Webber, *Discrete Contin. Dyn. Syst., Ser. B* **3**, 589 (2003).
  - [11] E. Pitman, C. Nichita, A. Patra, A. Bauer, M. Sheridan, and M. Bursik, *Phys. Fluids* **15**, 3638 (2003).
  - [12] R. Denlinger and R. Iverson, *J. Geophys. Res.* **109**, F01014 (2004).
  - [13] F. Bouchut, A. Mangeney-Castelnaud, B. Perthame, and J.-P. Vilotte, *C. R. Acad. Sci., Ser. I: Math.* **336**, 531 (2003).
  - [14] S. P. Pudasaini, Y. Wang, L.-T. Sheng, S.-S. Hsiau, K. Hutter, and R. Katzenbach, *Phys. Fluids* **20**, 073302 (2008).
  - [15] S. P. Pudasaini and K. Hutter, *J. Fluid Mech.* **495**, 193 (2003).
  - [16] J. M. N. T. Gray, M. Wieland, and K. Hutter, *Proc. R. Soc. London, Ser. A* **455**, 1841 (1999).
  - [17] S. B. Savage and K. Hutter, *J. Fluid Mech.* **199**, 177 (1989).
  - [18] Y. C. Tai, S. Noelle, J. Gray, and K. Hutter, *J. Comput. Phys.* **175**, 269 (2002).
  - [19] R. J. LeVeque, *Numerical Methods for Conservation Laws* (ETH Zurich, Birkhauser-Verlag, Basel, 1990).
  - [20] C. Ancey, *J. Non-Newtonian Fluid Mech.* **142**, 4 (2007).
  - [21] P. Jop, Y. Forterre, and O. Pouliquen, *Nature (London)* **441**, 727 (2006).
  - [22] M. E. Eglit, *Advances in Mechanics and the Flow of Granular Materials*, edited by M. Shahinpoor (Clausthal-Zellerfeld and Gulf Publishing Company, Houston, TX 1983), Vol. 2, p. 577.

- [23] F. Chevoir, M. Prochnow, J. T. Jenkins, and P. Mills, in *Powder and grains*, edited by Y. Kishino (Balkem, Lisse, 2001).
- [24] S. C. du Pont, P. Gondret, B. Perrin, and M. Rabaud, *Europhys. Lett.* **61**, 492 (2003).
- [25] GDR MiDi, *Eur. Phys. J. E* **14**, 341 (2004).
- [26] F. Chevoir, F. D. Cruz, M. Prochnow, P. Rognon, and J. N. Roux, *17th ASCE Engineering Mechanics Conference* (University of Delaware, Newark, DE, 2004).
- [27] Y. Wang, H. Hutter, and S. P. Pudasaini, *J. Appl. Math. Mech.* **84**, 507 (2004).
- [28] S. P. Pudasaini, S.-S. Hsiau, Y. Wang, and K. Hutter, *Phys. Fluids* **17**, 093301 (2005).
- [29] S. P. Pudasaini, Y. Wang, and K. Hutter, *Philos. Trans. R. Soc. London, Ser. A* **363**, 1551 (2005).
- [30] S. P. Pudasaini, Y. Wang, and K. Hutter, *Nat. Hazards Earth Syst. Sci.* **5**, 799 (2005).
- [31] F. Bouchut and M. Westdickenberg, *Commun. Math. Sci.* **2**, 359 (2004).
- [32] R. R. Kerswell, *Phys. Fluids* **17**, 057101 (2005).
- [33] A. Mangeney, P. Heinrich, and R. Roche, *Pure Appl. Geophys.* **157**, 1081 (2000).
- [34] I. Luca, Y. C. Tai, and C. Y. Kuo, *Math. Models Meth. Appl. Sci.* (to be published).
- [35] I. Luca, K. Hutter, Y. C. Tai, and C. Y. Kuo (unpublished).
- [36] Y. Tai and C. Kuo, *Acta Mech.* **199**, 71 (2008).
- [37] O. Pouliquen and Y. Forterre, *J. Fluid Mech.* **453**, 133 (2002).